

A mid-infrared study of very low mass stars and brown dwarfs in Upper Scorpius [★]

H. Bouy^{1,3,★★}, N. Huélamo^{2,5}, E. L. Martín³, D. Barrado y Navascués⁴, M. Sterzik⁵, and E. Pantin⁶

¹ Astronomy Department, University of California, Berkeley, CA 94720, USA
e-mail: hbouy@astro.berkeley.edu

² Observatório Astronómico de Lisboa, Tapada da Ajuda, 1349-018 Lisboa, Portugal
e-mail: nhuelamo@oal.ul.pt

³ Instituto de Astrofísica de Canarias, C/ Vía Láctea s/n, 38200 La Laguna, Tenerife, Spain
e-mail: ege@iac.es

⁴ Laboratorio de Astrofísica Espacial y Física Fundamental (LAEFF-INTA), Apdo 50727, 28080 Madrid, Spain
e-mail: barrado@laeff.inta.es

⁵ European Southern Observatory, Casilla 19001, Santiago 19, Chile
e-mail: msterzik@eso.org

⁶ Services d'Astrophysique, Saclay CEA, 91191 Gif-sur-Yvette, France
e-mail: pantin@sapvzg.saclay.cea.fr

Received 24 July 2006 / Accepted 20 August 2006

ABSTRACT

Context. To investigate the formation of sub-stellar objects, we observed a sample of ultracool dwarf members of the Upper Scorpius OB association.

Aims. The properties of disks, such as their composition, life-time, and frequency compared to the accretor frequency, provide important clues to the mechanisms responsible for the formation of stellar and sub-stellar objects.

Methods. We report the results of mid-IR observations with VISIR at the VLT of 10 ultracool dwarf members of the nearby Upper Scorpius OB association in four filters ranging from 8.59 (PAH1) to 12.8 μm (Ne II) and one brown dwarf observed with Spitzer between 3.6 and 24 μm .

Results. Seven of our targets were detected in at least one of the bands, and we derived upper limits on the fluxes of the remaining 4. These results combined with previous studies from the literature lead to an improved disk frequency of $50 \pm 12\%$. This frequency is significantly higher than for accretors ($16.3\% \pm 6.2\%$). Only one object showing mid-IR excess also has $H\alpha$ emission at a level that indicates it must be accreting. Four of the detected targets are multiple system candidates.

Conclusions. The observed disk frequency for sub-stellar objects in the Upper Scorpius association is similar to that of stars, consistent with a common formation scenario. It is also similar to the disk fractions observed in younger clusters, suggesting that the disk lifetimes might be longer for ultracool dwarfs than for higher-mass stars.

Key words. stars: formation – stars: low mass, brown dwarfs – accretion, accretion disks

1. Introduction

Over the past ten years, a large number of brown dwarfs (BD) and very low-mass stars have been discovered in the field, in star-forming regions and in clusters. One of the most debated questions is whether sub-stellar objects form the same way as stars do, via the fragmentation and collapse of a molecular cloud, or as aborted stellar embryos ejected from their parent proto-stellar cluster. A comparison of stellar and sub-stellar disk properties directly addresses this question and provides crucial information and straightforward constraints on the models of formation.

The first evidence showing that brown dwarfs have disks was given several years ago (Luhman & Rieke 1999; Comeron et al. 1998), and since then substantial fractions of young brown dwarfs in star-forming regions have been reported to have circumstellar material (see e.g. Luhman et al. 2005a,b,c; Mohanty et al. 2005b; Sterzik et al. 2004; Jayawardhana et al. 2003;

Liu et al. 2003; Muench et al. 2001; Natta & Testi 2001) and to undergo an accretion phase (e.g. Jayawardhana et al. 2002; Natta et al. 2004; Barrado y Navascués et al. 2004; Mohanty et al. 2005b; Muzerolle et al. 2005). From their near-IR observations, Jayawardhana et al. (2003) estimates an initial frequency of disk around BD and very low-mass stars of $50\% \pm 25\%$ in various star-forming regions. Using Spitzer to study the population of the IC348 young cluster, Lada et al. (2006) estimates disk fractions of 47% for K6–M2 stars and 28% for M2–M6 stars, while Luhman et al. (2005c) reports 42% for members later than M6. Although these results seem to show that BD originate more like stars than like ejected or evaporated embryos, our understanding of the formation processes is far from complete. It is still unclear whether one mechanism eventually prevails over the others, and how the contribution of each mechanism to the overall final population depends on the environment and initial conditions.

The Upper Scorpius OB association (hereafter USco) is an ideal place in which to study the properties of ultracool dwarf disks. It is close and young enough (145 pc and 5 Myr, de Zeeuw et al. 1999) that even its sub-stellar members have relatively

* Based on observations made with ESO Telescopes at the Paranal Observatories under program ID 075.C-0148.

** Marie Curie Outgoing International Fellow.

Table 1. List of targets.

Target	RA (J2000)	Dec (J2000)	SpT
DENIS155556	15 55 56.0	-20 45 18.5	M6.5
DENIS160334	16 03 34.7	-18 29 30.4	M5.5
DENIS160514	16 05 14.0	-24 06 52.6	M6.0
DENIS160603	16 06 03.9	-20 56 44.6	M7.5
DENIS160951	16 09 51.1	-27 22 42.2	M6.0
DENIS160958AB ¹	16 09 58.5	-23 45 18.6	M6.5
DENIS161050	16 10 50.0	-22 12 51.8	M5.5
DENIS161816AB ¹	16 18 16.2	-26 19 08.1	M5.5
DENIS161833AB ¹	16 18 33.2	-25 17 50.4	M6.0
DENIS161939AB ¹	16 19 39.8	-21 45 35.1	M7.0
DENIS162041 ²	16 20 41.5	-24 25 49.0	M7.5

¹ Multiple systems (Bouy et al. 2006; Luhman 2005)

² Observed with Spitzer rather than VISIR

Notes. Coordinates and spectral types from Martín et al. (2004).

bright luminosities, and the sample of known sub-stellar members is one of the largest for that type of association. Moreover, by comparing the disk properties of the 5 Myr USco to those of younger associations such as IC348 (Lada et al. 2006; Luhman et al. 2005c) or Cha I (Luhman et al. 2005c), it is possible to study the disk evolution and lifetimes. We have obtained mid-infrared (mid-IR) photometry for 10 ultracool dwarf members of the association using VISIR on the VLT, and retrieved mid-IR photometry of an additional USco brown dwarf from the Spitzer public archive. In Sect. 2, we describe the observations, data reduction, and analysis, and in Sect. 3, we discuss the derived disk frequency and compare it to previous studies.

2. Observations and data reduction

The original sample consists of 11 ultracool dwarfs with H α emission in USco, as reported by Martín et al. (2004). Table 1 gives a summary of the targets' properties. All have been spectroscopically confirmed as ultracool dwarfs and as member of the Upper Sco association. Two of the targets were classified as accretors by Martín et al. (2004) on the basis of their H α emission and the saturation criterion defined by Barrado y Navascués & Martín (2003) (see Table 2). Four of the targets were recently resolved as multiple system candidates by Bouy et al. (2006) and Luhman (2005). One of them (DENIS161833) has been confirmed as a physical pair by the last two authors, while second-epoch observations are still going-on to confirm the multiplicity of the other ones.

2.1. VISIR observations

Our mid-IR observations were obtained with VISIR, the mid-IR instrument mounted on the Cassegrain focus of Melipal (UT3) at the VLT (Lagage et al. 2004). The selected pixel-scale, 0".075, results in a total field of view of 19".2 \times 19".2 on its 256 \times 256 BIB detector. The observations were performed using standard chopping and nodding techniques in order to suppress the sky emission. The chopping throws were selected between 8–10". A standard star was observed before and/or after each target with the same configuration and at a similar airmass. The targets were observed with the PAH1, PAH2, SIV and NeII filters, where the instrument has its best sensitivity. The effective wavelengths of these filters are described in Table 3.

Table 2. Disk, accretion and multiplicity, of the targets.

Target	Mid-IR Excess	Accretion	Companion
DENIS-PJ155556	yes	no	no
DENIS-PJ160334	yes	no	yes? ^a
DENIS-PJ160514	...	no	no
DENIS-PJ160603	...	yes	no
DENIS-PJ160951	...	no	no
DENIS-PJ160958	no	no	yes (12 AU)
DENIS-PJ161050	no	no	yes? ^a
DENIS-PJ161816	no	no	yes (21 AU)
DENIS-PJ161833	no	no	yes (134 AU)
DENIS-PJ161939	yes	yes	yes (26 AU)
DENIS-PJ162041	no ^b	no	no

^a As discussed in the text, we infer the possible multiplicity of DENIS-PJ160334.7-182930 and DENIS-PJ161050.0-221252 from their SEDs, but these were not resolved with adaptive optics.

^b Observed with Spitzer rather than VISIR.

Note. Accretion diagnostic from Martín et al. (2004). “No companion” means no companion resolved at separations ≥ 5 AU and $\Delta\text{Mag}(K_s) < 2$ mag (Bouy et al. 2006; Bouy et al. 2007, in prep.).

Table 3. Effective wavelengths and bandwidths of the VISIR filters used for this study.

Filter	λ_0 [μm]	$\Delta\lambda$ [μm]
PAH1	8.59	0.42
SIV	10.49	0.16
PAH2	11.26	0.59
NeII	12.81	0.21

The data were processed with a customary pipeline based on IDL (Interactive Data Language) routines. The pipeline includes bad pixel correction and the shift-and-add technique for the individual frames, each of them corresponding to a chopping position (Pantin et al. 2005). Table 4 shows a summary of the observations, and Fig. 1 shows a sample of four of the images we obtained.

2.2. Spitzer archival data

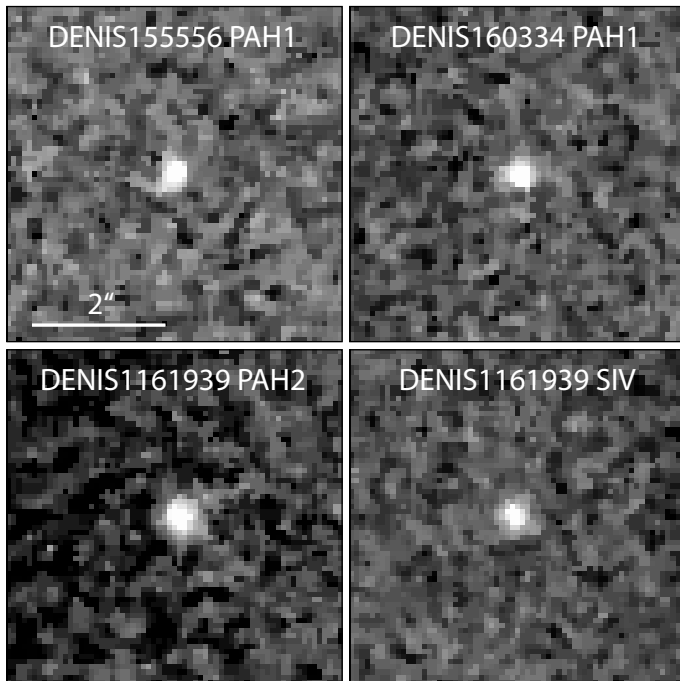
In order to complement our ground-based survey, we searched the Spitzer public archive for observations of USco brown dwarfs. Only one object of the Martín et al. (2004) sample, the M7.5 brown dwarf DENIS-PJ162041.5-242549.0, had been observed in the course of a public survey. It fell in both the IRAC and MIPS pointings of the “C2d continued” legacy survey (Program 177, P.I. N. Evans). The object had been observed twice in each of the IRAC and MIPS bands, and is detected only in the IRAC images (see Fig. 2).

2.3. Analysis of the data

Most of the VISIR detections are so faint that only the central overlay of the two positive beams can be used for photometry. Aperture photometry was performed using standard procedures under IDL with the APPHOT library. An optimized aperture was derived using the curve-of-growth method. Since the targets are faint, the best aperture was chosen to maximize the signal-to-noise ratio on the standard stars' curves of growth. The derived apertures were then used to measure the count-rate of each associated target. Uncertainties were estimated measuring the background noise weighted over the aperture. The count rates were

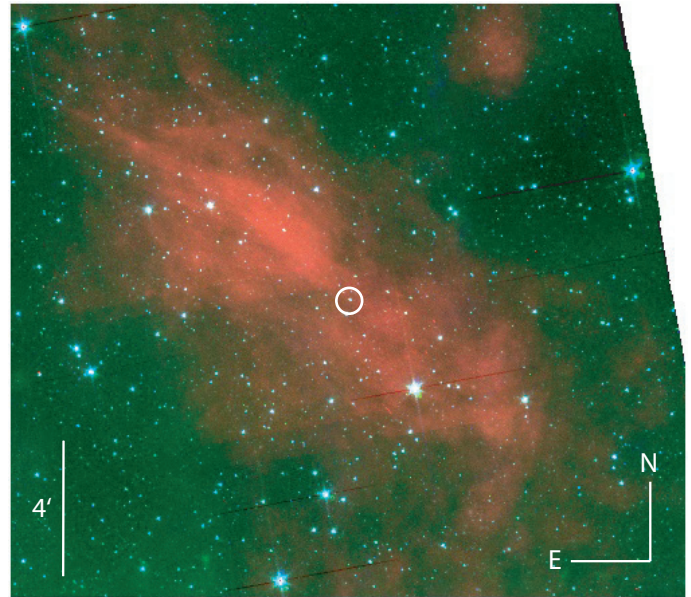
Table 4. Observation Log.

Target	Filter	Exp. time [s]	Calibrator
30/05/2005			
DENIS161816	PAH1	3600	HD145897
DENIS161833	PAH2	3600	HD145897
DENIS160334	PAH2	3600	HD168592
DENIS160514	PAH2	3600	HD168592
DENIS160958	PAH2	3600	HD152880
31/05/2005			
DENIS161816	PAH2	3600	HD145897
DENIS161939	PAH2	3600	HD145897
DENIS160603	PAH2	3600	HD146791
DENIS160951	PAH2	3600	HD146791
DENIS161050	PAH2	3600	HD152880
DENIS155556	PAH2	3600	HD152880
01/06/2005			
DENIS161939	PAH1	3600	HD151249
DENIS161939	SIV	3600	HD151249
DENIS160334	SIV	3600	HD179886
DENIS160334	PAH1	3600	HD156277
DENIS160603	PAH2	3600	HD138538
02/06/2005			
DENIS155556	PAH1	3600	HD133774
DENIS155556	SIV	3600	HD133774
DENIS161939	NEII	1800	HD152880

**Fig. 1.** VISIR image stamps of DENIS155556, DENIS160334, and DENIS161939. The scale and the filter are indicated.

then translated into fluxes using the calibrated fluxes of the standard stars (Cohen et al. 1992, 1995, 1996; Cohen & Davies 1995) provided by the VISIR team. The results are shown in Table 5 and in Fig. 3.

We measured the IRAC fluxes of DENIS162041 using a recommended aperture of 5 pixels, a sky annulus between 5 and 10 pixels, and aperture corrections of 1.061, 1.064, 1.067, and 1.089 for the four channels, respectively, as provided in the IRAC Data Handbook. We derived the final fluxes and their uncertainties by computing the average and the deviation of the

**Fig. 2.** Three-color image obtained using the Spitzer IRAC images at 3.6, 4.5, and 8.0 μm (blue, green, red, respectively). The scale and orientation are indicated. DENIS162041 is indicated with a white circle. It is located in a region of higher extinction.

two consecutive measurements. The 5.8 μm flux has larger uncertainties because the object fell at the edge of a dither pattern, and the PSF of the object appears slightly degraded. To estimate an upper limit at 24 μm , we measured the flux within an aperture of 14 pixels ($\sim 35''$) at nine positions centered on the expected location of the source, and derived the final upper limit from the 3- σ standard deviation of the nine measurements. Table 6 gives the photometry of this object, and Fig. 4 shows its SED.

3. Analysis

Figure 3 shows the spectral energy distributions (SED) of the VISIR targets and compares them to the relevant DUSTY atmospheric model SEDs from Allard et al. (2001) and to the λ -Ori M dwarfs from Barrado y Navascués (2007), corrected for the distance of the association. For the comparison, we used the effective temperature scale derived for USco members by Mohanty et al. (2004). This figure shows that three among the six targets detected in our mid-IR images display a significant excess (DENIS155556, DENIS160334, DENIS161939). Four sources (DENIS161833, DENIS161816, DENIS161050, and DENIS160958) show detections or upper limits very close to the photospheric values. Finally, the three sources left (DENIS161603, DENIS160514, DENIS160951) were not detected and the derived upper limits are so much larger than the photospheric values that we cannot draw any conclusion regarding the presence or absence of circumstellar disks around them.

Figure 4 shows the SED of DENIS162041. There is a clear discrepancy between the SED and the DUSTY model/comparison M dwarf SEDs. The fluxes are lower than expected, with the difference increasing toward bluer wavelengths, suggesting that the discrepancy might be due to reddening. The Spitzer images show that DENIS162041 is indeed located in an area where extinction is relatively high, as shown in Fig. 2, and a much better fit of the SED is obtained when unreddening the SED with $A_V = 3.3$, assuming a standard reddening law as

Table 5. Photometry of the targets.

Target	<i>I</i>	<i>J</i>	<i>H</i>	<i>K</i>	PAH1	SIV	PAH2	NeII
DENIS-PJ155556.0-204518	0.82	7.07	7.72	10.41	4.6 ± 0.7	<6.5	2.4 ± 1.0	...
DENIS-PJ160334.7-182930	2.60	17.14	18.96	16.56	5.4 ± 0.9	6.3 ± 3.4	4.9 ± 1.2	...
DENIS-PJ160514.0-240652	1.83	12.89	12.15	10.36	<3.2	...
DENIS-PJ160603.9-205644	0.63	6.38	7.04	7.00	<6.3	...
DENIS-PJ160951.1-272242	1.20	7.76	8.19	7.28	<4.5	...
DENIS-PJ160958.5-234518AB	2.04	14.42	16.29	15.73	3.1 ± 1.4	...
DENIS-PJ161050.0-221252	2.15	14.15	15.00	13.69	<2.7	...
DENIS-PJ161816.2-261908AB	3.26	21.95	30.47	27.11	2.9 ± 0.9	...	<29.1	...
DENIS-PJ161833.2-251750AB	2.19	16.52	21.22	20.13	2.4 ± 1.0	...
DENIS-PJ161939.8-214535AB	1.24	9.47	9.90	9.17	6.9 ± 1.0	8.0 ± 1.4	9.6 ± 1.2	<10.7

Note. *I* fluxes from DENIS magnitudes; *J*, *H*, and *K* fluxes from 2MASS magnitudes. All fluxes in mJy, 1- σ uncertainties and 3- σ upper limits were derived as described in the text. DENIS161833AB was the only binary in the sample that could have been resolved with VISIR, but we detect only one of the components.

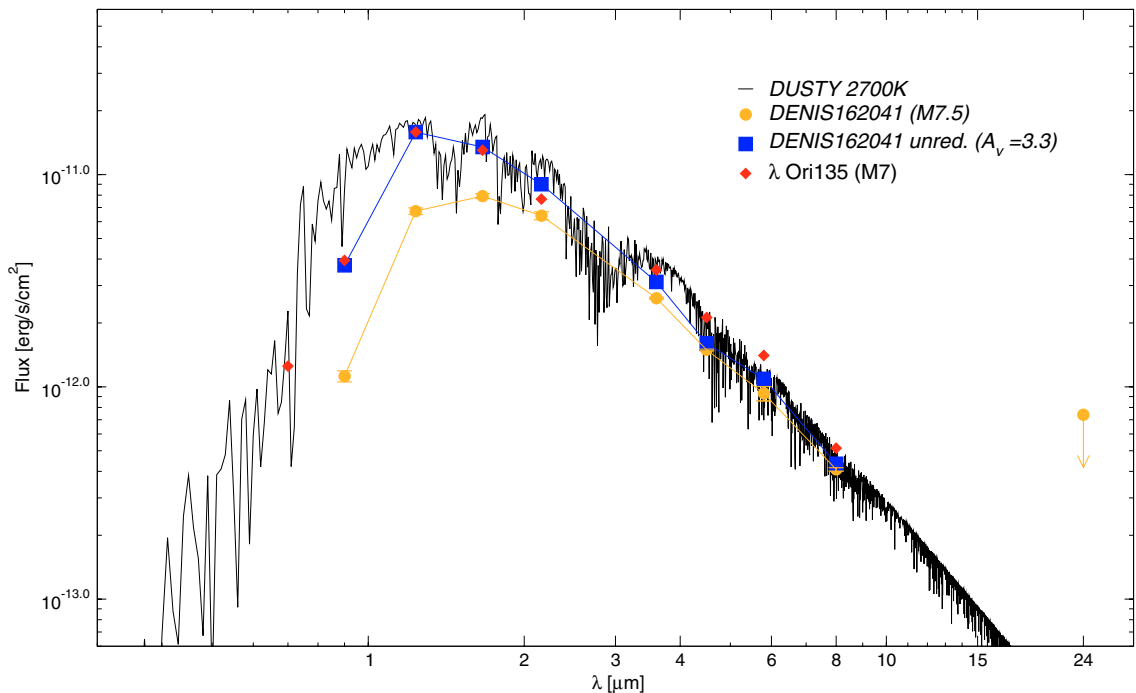


Fig. 3. Spectral energy distributions of the 10 VISIR targets (black circles). Upper limits are indicated with arrows and connected with dotted lines. DUSTY atmospheric models (with the indicated T_{eff} and $\log(g) = 4.0$, Allard et al. 2001) and SEDs of λ -Ori M dwarfs (red diamonds) of similar spectral types from Barrado y Navascués (2007) corrected for the distance of the association are over-plotted for comparison. The T_{eff} were chosen according to Mohanty et al. (2004) Spectral type vs. T_{eff} scale for USco objects. The individual components of the 4 known binary systems having similar masses (see Bouy et al. 2006), their SEDs are compared to the sum of two atmospheric models/ λ -Ori M dwarfs of the same effective temperature. Two objects (DENIS161050 and DENIS160334) are twice brighter than the atmospheric models corresponding to their effective temperatures. The orange curves show the comparison with the sum of two atmospheric models of the same temperature, suggesting these targets might be unresolved binaries (see discussion in the text).

given in Rieke & Lebofsky (1985). In any case, DENIS162041 does not display any mid-IR excess.

3.1. Inner disks and multiple systems

Recent studies have found a significant fraction of very low-mass star and brown dwarf multiple systems in star forming regions (between 9–33% for separations greater than 4 AU in Taurus and USco, Bouy et al. 2006; Kraus et al. 2006, 2005), and several young multiple systems exhibit evidence of disks and/or accretion (Chauvin et al. 2005; Bouy et al. 2004; Sterzik et al. 2004). As in the case of stars, the formation of multiple systems surrounded by disk(s) seems to be a relatively common outcome of sub-stellar formation. Among the four known multiple systems

detected in our VISIR images, only DENIS161939AB shows a clear mid-IR excess indicating the presence of an inner disk. This binary has a separation of $0'.177$ (Bouy et al. 2006), or 26 AU at the distance of USco, and the unresolved system was classified as an accretor by Martín et al. (2004). DENIS161833AB was the only binary in the sample that could have been resolved with VISIR, but we only detect one of the members.

Two targets (DENIS161050 and DENIS160334) are brighter by a factor of 2 than the atmospheric models with the effective temperature corresponding to their spectral types. Two explanations can be given: either the targets are unresolved binaries, and/or they lie closer to the Sun than the rest of the targets. Figure 3 shows that the fit becomes very good if one simply considers that these objects are unresolved binaries and

Table 6. Photometry of DENIS-PJ162041.5-242549.0 .

Band	Flux
<i>I</i>	0.26 ± 0.02
<i>J</i>	2.77 ± 0.10
<i>H</i>	4.39 ± 0.12
<i>K</i>	4.61 ± 0.20
$3.6 \mu\text{m}$	3.14 ± 0.03
$4.5 \mu\text{m}$	2.24 ± 0.02
$5.8 \mu\text{m}$	1.80 ± 0.14
$8.0 \mu\text{m}$	1.09 ± 0.02
$24.0 \mu\text{m}$	<5.9

Note. *I* flux from DENIS magnitude; *J*, *H*, and *K* fluxes from 2MASS magnitudes. All fluxes in mJy, uncertainties, and $3\text{-}\sigma$ upper limits derived as described in the text.

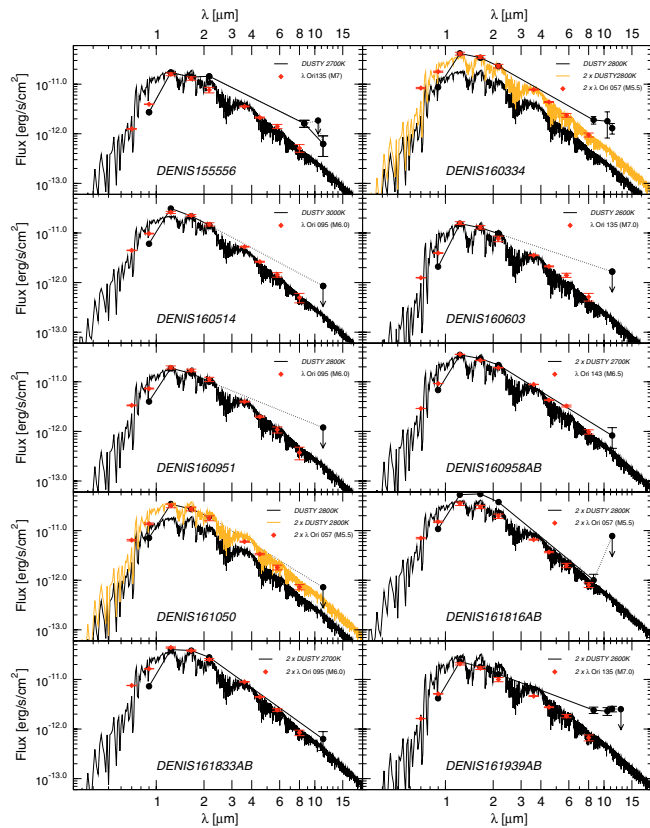


Fig. 4. Spectral energy distributions of DENIS162041. The SED of DENIS162041 (orange) does not fit the corresponding model (black line) or comparison M7 dwarf (red diamonds). The deviation is increasing towards bluer wavelengths, suggesting that the object suffers from extinction. The SED fits relatively well the model/comparison M7 dwarf after unreddening with $A_V = 3.3$ (blue squares). The object does not show any excess in the mid-IR.

compares their SED with the sum of two atmospheric models of the same temperature. This assumes that the two components would have similar effective temperatures, as suggested by the results of Bouy et al. (2006)s showing that all resolved very low-mass and BD USco binaries have close to equal mass ratios. These objects were not resolved in the high angular-resolution observations of Bouy et al. (2006). If multiples, the companions must therefore be at separations <5 AU and/or $\Delta\text{Mag}(K_s) > 2$ mag. The data could be equally well-fitted with a single

theoretical SED only $\sqrt{2}$ closer to the Sun than the rest of the sample (which would place them at ~ 100 pc). Martín (1998) indeed shows that members of the USco association can be found as close as 80 pc from the Sun.

In either case, the SED of DENIS161050 do not show any significant excess, while that of DENIS160334 displays a substantial excess at wavelengths greater than $8 \mu\text{m}$.

3.2. Disk fraction

Three objects (DENIS155556, DENIS160334, and DENIS161939AB) among the six with mid-IR detections (the latter three plus DENIS160958, DENIS161816AB, and DENIS161833AB) show a clear excess at $8 \mu\text{m}$ and above. DENIS162041 was detected in the Spitzer images but would not have been detected in our ground-based survey. We therefore do not include it in the following discussion. The upper limit on DENIS161050 mid-IR flux is only a factor of <2 above the atmosphere, and the presence of disk can be ruled out at a relatively high confidence level. Martín et al. (2004) classified DENIS160603 as an accretor on the basis of its strong $H\alpha$ emission ($W(H\alpha) = 105 \pm 12 \text{ \AA}$). We did not detect this object in our mid-IR images but the upper limit on its mid-IR flux is too high to put any valuable constraints on the presence or absence of circumstellar material. If we assume that we did not detect this object because of the limited sensitivity of our images, we can add it to the statistics and obtain a disk frequency¹ of $50\% \pm 16\%$ (4 disks over 8 targets). The remaining two upper limits (for DENIS160514 and DENIS160951) are too high to be conclusive so we do not include these objects in the statistics.

The disk frequency estimated above is consistent with what is reported by Jayawardhana et al. (2003) using *L*-band photometry (4 disks among 8 targets, $50\% \pm 16\%$, with uncertainties recomputed as described previously). Since their sample does not overlap with the one presented here, and although their study was performed using a different technique, one can tentatively add the two samples to derive an improved disk fraction of $50\% \pm 12\%$ (8/16). This result is comparable to the one reported for Scorpius-Centaurus solar-mass stars, where Chen et al. (2005) recently reported a preliminary estimate of the disk fraction among F and G stars ($>35\%$) using Spitzer photometry.

3.3. Sub-stellar formation, disk evolution, and multiple systems

Table 2 summarizes the properties of multiplicity, disk, and accretion of the sample. The $10 \mu\text{m}$ excesses we observed are produced by rather warm dust (300 K) close to the object (<1 AU). We do not probe any outer disk, and cannot say anything about the presence of circumbinary material that would be located at distances larger than the separations of these systems. Neither can we tell whether only one or the two components have a disk, but this should not change our estimate of the disk fraction since binaries are counted as single objects anyway, assuming that the two components must be coeval.

Note also that these results consider that the inner disk frequency of multiple systems and single objects at the age of Upper Scorpius must be the same, or, in other words, that the presence of a companion at such separations does not affect the evolution of the disk(s) to the point that we would not have

¹ Deriving small number statistics, we estimate the uncertainties by constructing a probability distribution for the disk frequency given the total sample size and the number of disks in the sample.

detected it. This assumption seems reasonable considering the relatively large separations of these binaries (12, 21, 26, and 134 AU, see Table 2 and Bouy et al. 2006) compared to the typical sizes of BD disks to which we are sensitive with these mid-IR observations (1 AU, see e.g. Monin et al. 2006; Meeus et al. 2003, for a discussion about disk evolution in young binaries).

3.4. Disks and accretion

Only one (DENIS161939) of the two objects of our sample classified as accretors by Martín et al. (2004) is detected in our mid-IR images. As explained above, the mid-IR upper limit derived for the other one (DENIS160603) is inconclusive. The accretor frequency ($16.3\% \pm 6.2\%$) reported by Martín et al. (2004) seems to be substantially lower than the disk frequency at the age of USco, indicating that transition disks are much more numerous than accretion disks, which is consistent with the timescale of disk decay observed for young ultracool dwarf disks (Sterzik et al. 2004; Mohanty et al. 2005a).

While the dust contributes to a small fraction of the mass of the disk ($\sim 1\%$), it is the most essential ingredient governing the heating/cooling of the disk and, therefore ultimately, its physical and geometrical evolution. The dust consists mainly of silicate grains with strong emission features in the mid-IR around $9.3 \mu\text{m}$ and $11.3 \mu\text{m}$. In their recent study, Apai et al. (2005) show that these two silicate features provide unique diagnostics of the grain growth, crystallization, and dust settling in the disk. Unfortunately, because of the limited sampling of the SEDs and because of the coupled influence of grain sizes and dust geometry on the SED, the results we present here do not allow us to perform a detailed analysis of the disk geometry and grain sizes. Complementary observations with e.g. Spitzer are required before a more detailed comparison of the SEDs of the targets with mid-IR excesses to disk models can be made, but the current results nevertheless show that some of the Upper Scorpius ultracool dwarfs are undergoing similar stages of evolution to the Cha I objects observed by Apai et al. (2005).

4. Concluding remarks

We report mid-IR observations of 11 ultracool dwarfs that are members of the Upper Scorpius association. Seven of them were detected in at least one of the mid-IR images, and 3 show a clear excess indicating the presence of circumstellar material. The relatively high frequency of disks ($50 \pm 12\%$) found among Upper Scorpius ultracool dwarfs (5 Myr) is comparable to those reported by e.g. Jayawardhana et al. (2003) and Luhman et al. (2005c) for a variety of younger associations (1–2 Myr), possibly indicating that the timescales of disk decay are longer for ultracool dwarfs than for solar-mass stars. Although the sample we present is too small to draw any statistically meaningful conclusion, there seems to be no significant difference between the disk frequency of single and multiple ultracool dwarfs. Since these relatively wide systems have most likely formed like stars (they are indeed very unlikely to have survived a gravitational ejection), this similarity between single and multiple objects might be an additional clue that most ultracool dwarfs must form like stars rather than ejected embryos. Further studies on larger samples of single and multiple systems are required to confirm these observations. Finally, only one of the objects displaying mid-IR excess also shows evidence of accretion, indicating that the frequency of transition disks in Upper Scorpius must be significantly higher than that of accretion disks.

Acknowledgements. We thank our referee, Kevin Luhman, for his prompt review and interesting comments that helped improve the manuscript. H. Bouy thanks the telescope operators and the support astronomers, as well as the whole Paranal SciOps team for their efficient support. H. Bouy acknowledges the funding from the European Commission's Sixth Framework Program as a Marie Curie Outgoing International Fellow (MOIF-CT-2005-8389).

This work is based on observations collected at the European Southern Observatory (Paranal, Chile), program 075.C-0148, P.I. Bouy. This work made use of the CDS VizieR on-line tools (Ochsenbein et al. 2000). This work makes use of DENIS data. The DENIS project has been partly funded by the SCIENCE and the HCM plans of the European Commission under grants CT920791 and CT940627. It is supported by INSU, MEN, and the CNRS in France, by the State of Baden-Württemberg in Germany, by DGICYT in Spain, by the CNR in Italy, by FFwFBWF in Austria, by FAPESP in Brazil, by OTKA grants F-4239 and F-013990 in Hungary, and by the ESO C&EE grant A-04-046. This publication made use of data products from the Two Micron All Sky Survey, which is a joint project of the University of Massachusetts and the Infrared Processing and Analysis Center/California Institute of Technology, funded by the National Aeronautics and Space Administration and the National Science Foundation.

References

- Allard, F., Hauschildt, P. H., Alexander, D. R., Tamanai, A., & Schweitzer, A. 2001, *ApJ*, 556, 357
- Apai, D., Pascucci, I., Bouwman, J., et al. 2005, *Science*, 310, 834
- Barrado y Navascués, D. & Martín, E. L. 2003, *AJ*, 126, 2997
- Barrado y Navascués, D., Mohanty, S., & Jayawardhana, R. 2004, *ApJ*, 604, 284
- Barrado y Navascués, D. et al. 2007, in prep.
- Bouy, H., Brandner, W., Martín, E. L., et al. 2004, *A&A*, 424, 213
- Bouy, H., Martín, E. L., Brandner, W., et al. 2006, *A&A*, 451, 177
- Bouy, H. et al. 2007, in prep.
- Chauvin, G., Lagrange, A. M., Dumas, C., et al. 2005, in *Protostars and Planets V*, 8329
- Chen, C. H., Jura, M., Gordon, K. D., & Blaylock, M. 2005, *ApJ*, 623, 493
- Cohen, M. & Davies, J. K. 1995, *MNRAS*, 276, 715
- Cohen, M., Walker, R. G., Barlow, M. J., & Deacon, J. R. 1992, *AJ*, 104, 1650
- Cohen, M., Witteborn, F. C., Bregman, J. D., et al. 1996, *AJ*, 112, 241
- Cohen, M., Witteborn, F. C., Walker, R. G., Bregman, J. D., & Wooden, D. H. 1995, *AJ*, 110, 275
- Comeron, F., Rieke, G. H., Claes, P., Torra, J., & Laureijs, R. J. 1998, *A&A*, 335, 522
- de Zeeuw, P. T., Hoogerwerf, R., de Bruijne, J. H. J., Brown, A. G. A., & Blaauw, A. 1999, *AJ*, 117, 354
- Jayawardhana, R., Mohanty, S., & Basri, G. 2002, *ApJ*, 578, L141
- Jayawardhana, R., Ardila, D. R., Stelzer, B., & Haisch, K. E. 2003, *AJ*, 126, 1515
- Kraus, A. L., White, R. J., & Hillenbrand, L. A. 2005, *ApJ*, 633, 452
- Kraus, A. L., White, R. J., & Hillenbrand, L. A. 2006, *ArXiv Astrophysics e-prints*
- Lada, C. J., Muench, A. A., Luhman, K. L., et al. 2006, *AJ*, 131, 1574
- Lagage, P. O., Pel, J. W., Authier, M., et al. 2004, *The Messenger*, 117, 12
- Liu, M. C., Najita, J., & Tokunaga, A. T. 2003, *ApJ*, 585, 372
- Luhman, K. L. 2005, *ApJ*, 633, L41
- Luhman, K. L. & Rieke, G. H. 1999, *ApJ*, 525, 440
- Luhman, K. L., Adame, L., D'Alessio, P., et al. 2005a, *ApJ*, 635, L93
- Luhman, K. L., D'Alessio, P., Calvet, N., et al. 2005b, *ApJ*, 620, L51
- Luhman, K. L., Lada, C. J., Hartmann, L., et al. 2005c, *ApJ*, 631, L69
- Martín, E. L. 1998, *AJ*, 115, 351
- Martín, E. L., Delfosse, X., & Guieu, S. 2004, *AJ*, 127, 449
- Meeus, G., Sterzik, M., Bouwman, J., & Natta, A. 2003, *A&A*, 409, L25
- Mohanty, S., Jayawardhana, R., & Basri, G. 2004, *ApJ*, 609, 885
- Mohanty, S., Jayawardhana, R., & Basri, G. 2005a, *Mem. Soc. Astron. It.*, 76, 303
- Mohanty, S., Jayawardhana, R., & Basri, G. 2005b, *ApJ*, 626, 498
- Monin, J., Clarke, C. J., Prato, L., & McCabe, C. 2006, *ArXiv Astrophysics e-prints*
- Muench, A. A., Alves, J., Lada, C. J., & Lada, E. A. 2001, *ApJ*, 558, L51
- Muzerolle, J., Luhman, K. L., Briceño, C., Hartmann, L., & Calvet, N. 2005, *ApJ*, 625, 906
- Natta, A. & Testi, L. 2001, *A&A*, 376, L22
- Natta, A., Testi, L., Muzerolle, J., et al. 2004, *A&A*, 424, 603
- Ochsenbein, F., Bauer, P., & Marcout, J. 2000, *A&AS*, 143, 23
- Pantin, E., Lagage, P.-O., Claret, A., et al. 2005, *The Messenger*, 119, 25
- Rieke, G. H. & Lebofsky, M. J. 1985, *ApJ*, 288, 618
- Sterzik, M. F., Pascucci, I., Apai, D., van der Blik, N., & Dullemond, C. P. 2004, *A&A*, 427, 245